Optical and Quantum Electronics manuscript No.
(will be inserted by the editor)

Asymmetrical Clipping Optical Filter Bank Multi-Carrier Modulation Scheme

Asmaa Ibrahim · Josep Prat · Tawfik Ismail

Received: date / Accepted: date

Abstract Filter bank multi-carrier (FBMC) is considered a promising alternative to the Orthogonal Frequency Division Multiplexing (OFDM) scheme. It improves spectral efficiency by eliminating the need for cyclic prefix while attenuating interference due to the robustness of the out-of-band emission. In this work, we present a framework, and the performance evaluation of FBMC is a multi-carrier modulation scheme for the direct detection of optical communications. As the proposed model has higher spectral efficiency than the classical ACO-OFDM, as removing the guard interval enhances the spectral efficiency. Furthermore, the perfect rectangular pulse shaping and eliminating the out of band emission of the filter bank enhances the ACO-FBMC the BER performance of the ACO-OFDM. We propose a transceiver model for Asymmetrical Clipped Optical FBMC (ACO-FBMC) based on Fast Fourier Transform (FFT) operations, analyze inter-frame interference, and offer an iterative receptive method to eliminate it. Finally, we compared the bit error rate (BER) performance of the ACO-FBMC using different overlapping factors with the ACO-OFDM.

Keywords 5G networks, Optical Wireless, Filter bank multi-carrier, Asymmetrical Clipped Optical, Orthogonal Frequency Division Multiplexing

1 INTRODUCTION

In this study, we investigate the physical layer of 5G networks challenges, such as bandwidth requirements, system costs, spread delay, and computational complexity of the remote radio heads (RRHs) that become trade-offs on the design process of the front-line transport network. In order to achieve this network flexibility, the cloud radio access network (CRAN) has been introduced, as it offers a solution by decentralizing the data plane and virtualize the network function. In CRAN architecture, the baseband function is pooled at the baseband unit (BBU) and allocated at the remote central office. Simultaneously, RRH, which represents the transceiver components, is distributed along with the cell, and connected to the BBU pool. In C-RAN, the fronthaul links such as optical fibers, free-space optic or mmWave that connect the BBU and RRH suffer from the capacity, latency, and level of intelligence of the network. This increases the development of wireless transport as a significant challenge for 5G network design. Many research types have identified the optical network as the best transport network for the 5G front-haul transport network, among many wired and wireless technologies. It offers a good compromise between low latency and high capacity even though the compatibility between the optical fronthaul as a transport network and the radio networks has to be carefully considered [1][2].

The multi-carrier modulation (MCM) techniques have been proved to have better spectral efficiency than the single carrier (SC) techniques on the physical layer level. Among MCM techniques, Orthogonal frequency division multiplexing (OFDM) dominates the current 4G network, enabling the convergence of the optical infrastructure with existing wireless networks [3]. These aspects proposed OFDM as the best candidate for the 5G optical transport network. Nevertheless, it suffers from inter-symbol interference (ISI) and a high peak to the average to power ratio (PAPR). This motivates researchers to investigate alternative MCM technique addresses the drawbacks of the classical OFDM.

Mainly MCM schemes can be classified at the structure level as MCM schemes can be categorized at the structural level into "orthogonal," "biorthogonal," and "non-orthogonal structures." Orthogonal patterns that adopt matched filter techniques with orthogonal base functions reduce spectral efficiency in OFDM zero padding (ZP). This eliminates the multipath effect by imposing a guard interval between OFDM symbols with a rectangular base function. Bi-orthogonal patterns are represented by an orthogonal base function on both sides, which contradicts the matched filter approach as the Cyclic Prefix (CP) OFDM. It causes a more extended rectangular shape base function on the transmitter of the

Asmaa Ibrahim ,Josep Prat
Department of Signal Theory and Communications, Universitat Politècnica de Catalunya, Barcelona, Spain

Tawfik Ismail (tismail@niles.cu.edu.eg)
National Institute of Laser Enhanced Sciences, Cairo University, Giza 12613, Egypt
Wireless Intelligent Networks Center (WINC), Nile University, Giza 12677, Egypt

This is a post-peer-review, pre-copyedit version of an article published in *Optical and quantum electronics*.
The final authenticated version is available online at: http://dx.doi.org/10.1007/s11082-021-02867-2

attached data. Finally, this analysis will incorporate non-orthogonal schemes that will be introduced throughout this paper.

In the front-haul network, the optical transport network, as mentioned above, the optical detection of OFDM/OQAM with RF subbands separated by the user is a promising scheme. It reduces interference and efficiently allocates bandwidth per user [4]. In the subject matter, presently, we are looking into OFDM/OQAM (Filter Bank Multi-carrier (FBMC)) for the front haul and studying its compatibility with the optical OFDM benchmarks. Our goal is to address the challenges of OFDM, including the high peak-to-average power ratio (PAPR) and the CP that occurs within optical networks with high spectral efficiency.

The main contribution of this paper is the first development, to the best of our knowledge, of the asymmetric clipping optical transceiver FBMC based on the Fast Fourier Transform (FFT). However, the authors use DC optical filter bank multi-carrier (DCO-FBMC in [5]. Their system is affected by the computational complexity of the corresponding filtering scheme and the high clipping noise. We also introduced an orthogonal dimension other than FBMC for RF systems. We then proposed spatial orthogonality between adjacent frames using odd indexed and even indexed asymmetrical optical clipping (ACO-FBMC). We modelled and eliminated the interframe clipping distortion using the iterative method on the receiver side..

2 SYSTEM MODEL

In this section, we illustrate the ACO-FBMC system model, as the transmitter and the design of the receiver are precisely proposed.

2.1 OQAM-FBMC

The general form of the OQAM-FBMC frames is shown in Fig. 1. The discrete baseband time OQAM signal can be written as

$$x(t) = \sum_{k=-\infty}^{\infty} \sum_{l=0}^{L-1} p_{l,k}(t) * X_{l,k} \tag{1}$$

where $X_{l,k}$ is the transmitted M-ary QAM signal at subcarrier l and time k, $p_{l,k}$ is the transmitted basis function where

$$p_{l,k} = p(t - KT) * e^{j2\pi lF(t-kT)} * e^{j\theta_{l,k}} \tag{2}$$

where F is the frequency and time k, unlike the OFDM, the OQAM system loses the complex orthogonality. Hence, the complex symbol's real and imaginary parts have to be separated into two frames [7]. IFFT Implementation of the FBMC system has been proposed in recent researches as an efficient implementation. In [6], the author proposed an IFFT implementation based on the overlap and add the scheme to shape each subcarrier of the OFDM symbol. In this technique the phase $\theta_{l,k}$ is chosen to be $(\pi/2)(l + k)$. Based on this implementation, the FBMC procedure will first perform IFFT for the QAM modulated symbols. Secondly, this frame will be repeated based on an arbitrary overlap factor O, representing the number of multicarrier symbols that overlap in the time domain, as shown in Fig. 2. Finally, the prototype filter is modified in combination with the repeated filter to reshape the FBMC frame subcarriers.

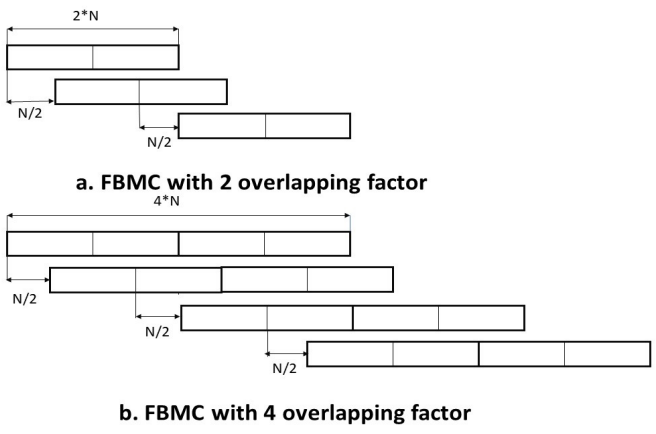

Fig. 1 OQAM-FBMC frames with 2 and 4 overlap factors

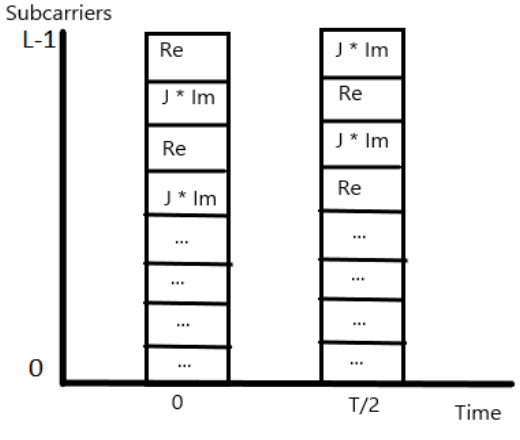

Fig. 2 OQAM-FBMC subcarriers

In OQAM-FBMC, multiple frames separated by the $T/2$ time shift send simultaneously. Implicitly, the first frame is carried by the real component, whereas the second frame is carried by the imaginary component of the transmitted signal, representing the phase orthogonality between the concurrently transmitted frames.

2.2 Transmitter Design

The block diagram of the ACO-FBMC transmitter is shown in Fig. 3, where the quadrature and in-phase components are processed separately and combined into an OQAM-FBMC symbol. The transmitter functionality is broken down into three main parts. First, OQAM is pre-processed, then combines the FBMC with the ACO scheme and, finally, clips the two components and transmits the shifted versions.

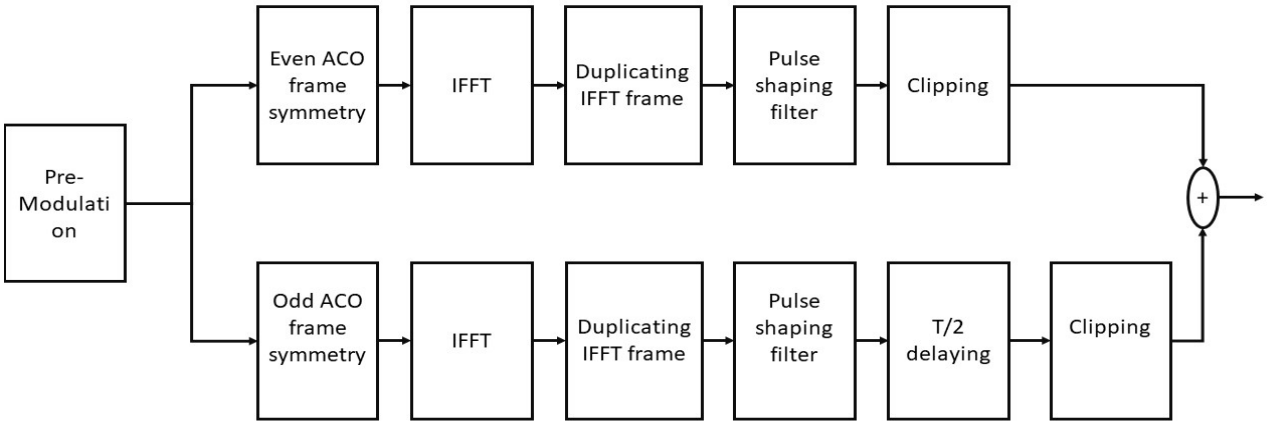

Fig. 3 OQAM-FBMC Transmitter

The typical bipolar OFDM signal modifies to be sent over intensity modulation with direct detection (IM/DD) optical system in the optical domain. As in IM/DD systems, the transmitted signal is modulated and carried by the optical carrier's intensity. Accordingly, this requires the optically transmitted signal to be pure real and positive valued. Many types of research over the past decade addressed this challenge and introduced the unipolar OFDM schemes. Several optical OFDM techniques have been developed as the direct current (DC) biased optical OFDM (DCO-OFDM) [8][10], the asymmetrically clipped optical OFDM (ACO-OFDM) [9][10].

These schemes are based on generating real baseband OFDM signal by enforcing the input signal to have Hermitian symmetry. In the DCO system, a DC component is appended to the real signal to produce a real positive valued signal, and then it is clipped to eliminate the negative parts. The added DC value is a challenge in the DCO system as it highly reduces the power efficiency of the DCO-OFDM scheme. In [5], DCO-FBMC has been proposed along with FBMC transceiver based on the matched filtering process. This system with a complex FBMC transmitter suffers from computational complexity and high clipping noise from eliminating negative parts. On the other hand, the ACO schemes are based on utilizing only the odd subcarriers and adding zeros on the even subcarriers. It has been shown that even subcarriers carry the clipping distortion [8]. The ACO-OFDM has high power efficiency and low spectral efficiency as only the odd subcarriers carry the data. Therefore, its spectral efficiency is half of the DCO-OFDM. The ACO-FBMC, dissimilar to the OQAM-FBMC, carries all the data on the only real component of the transmitted data. The clipping distortion affects the imaginary component of all transmitted subcarriers. Alternatively, another dimension of orthogonality has to be added to send multiple shifted frames simultaneously.

We propose a subcarrier orthogonality scheme to be implemented to ensure the orthogonality between the two components of the OQAM signal transmitted. In each frame sequence, the first frame will be sent over an odd indexed ACO according to (3), as shown in Fig. 4.

$$\begin{aligned} X\left(\frac{L}{2}+i+1\right) &= X\left(\frac{L}{2}-i+1\right) \quad \text{for odd } i \\ X(i) &= 0 \qquad\qquad\qquad\quad \text{for even } i \end{aligned} \tag{3}$$

Furthermore, the second frame will be sent over even indexed ACO according to (4) as shown in Fig. 5.

$$\begin{aligned} X\left(\frac{L-1}{2}-i\right) &= X\left(\frac{L+1}{2}-i\right) \qquad \text{for even } i \\ X(i) &= 0 \qquad\qquad\qquad \text{for odd } i,\ i=0,\frac{L-3}{2},\frac{L+1}{2} \end{aligned} \tag{4}$$

where i is the frame number.

Mapping the ACO scheme to the FBMC system discussed above produces the frames structures shown in Fig. 6. This structure verifies Hermitian symmetry, real output signal as both Frames are pure imaginary, and finally, it satisfies the OQAM-FBMC frame structure. Negative parts of the OFDM output frame will be clipped and transmitted over the optical device.

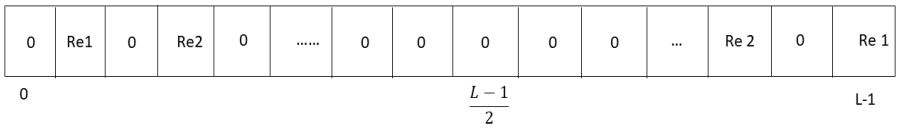

Fig. 4 Odd Indexed ACO frames

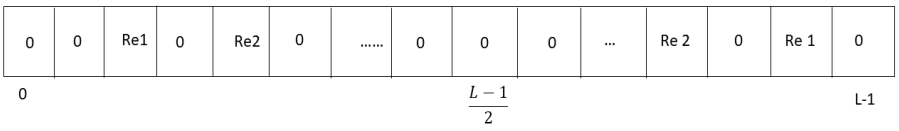

Fig. 5 Even Indexed ACO frames

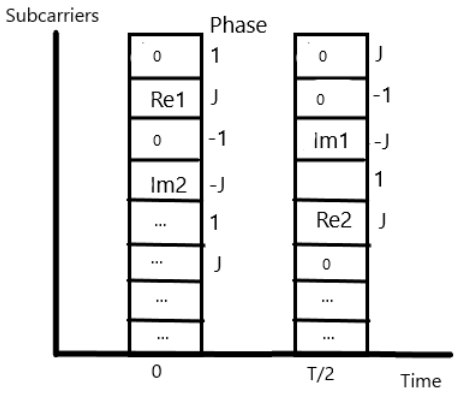

Fig. 6 ACO-FBMC frames

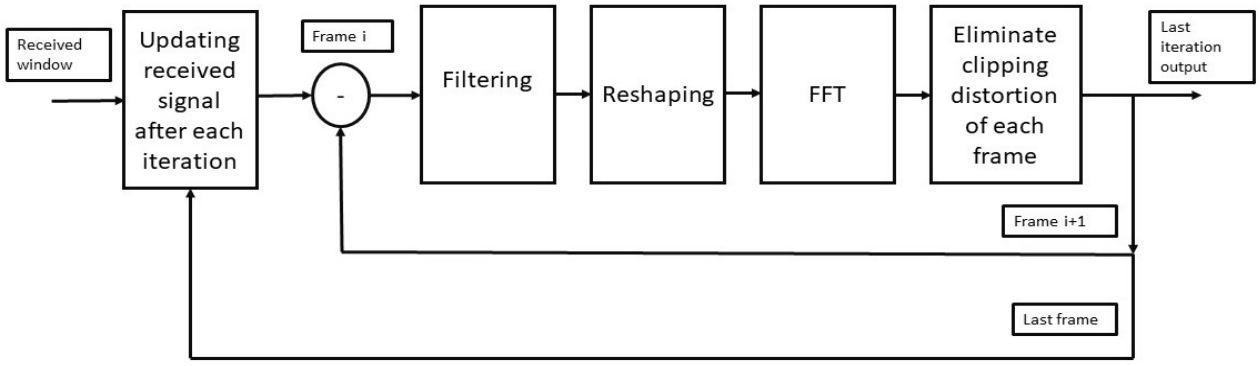

Fig. 7 OQAM-FBMC Receiver

2.3 Receiver Design

At the receiver shown in Fig. 7, the received signal is divided into windows, each of which is multiplied by a filter and reshaped to multiple segments with the size $T \times O$, where T is the symbol duration, and O is the overlapping factor — then FFT on the first window to produce the first received frame. Partially eliminating inter-frame interference is represented by regenerating the transmitted signal by performing IFFT on the first received frame to be subtracted from the total received frame. This process is repeated until the last frame has been detected.

These received frames are used in iterative manner to eliminate all the clipping distortion. Fig. 8 shows the receiver procedure.

3 INTERFERENCE ANALYSIS

The ACO-FBMC performance affected by the two sources of distortion inter frame interference and self-frame interference. Hard clipping of transmitted signal causes distortion on specific sub-carriers. The clipping distortion interfere with the data carried by the same frame and the data carried by the adjacent frames. In this section the clipping distortion and its effect on the data carried by the same frame is proposed. The FBMC-OQAM transmitted signal is

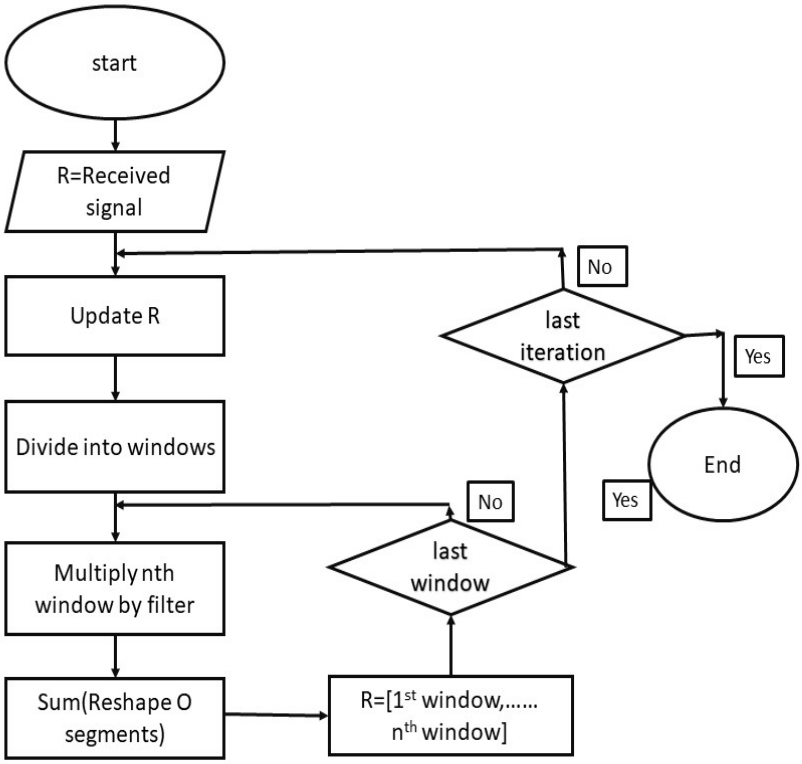

Fig. 8 The receiver procedure flow chart

introduced in (1) and $\theta_{l,k}$ is the phase to shift the interference to the imaginary domain and given by

$$\theta_{l,k} = \frac{\pi}{2} * (k + l) \tag{5}$$

For simplicity the clipping distortion is studied at k=0 for the odd ACO-FBMC frame ()

$$x_0(t) = p(t) * \sum_{l=0}^{L-1} e^{j2\pi lFt} * e^{j\frac{\pi}{2}*(l)} X_l \tag{6}$$

For discrete time signal $x(n) = x(nT)$

Reference to the Bussgang's theorem, the non linear effect of the clipping negative parts on the transmitted signal is represented as an additional distortion to the original signal [14]. So that, the received signal can be expressed as

$$X(l) = X_{clipped}(l) + D(l) \tag{7}$$

$$X_{clipped}(l) = \sum_{n=0x(n)>0}^{N-1} x(n)\, e^{-\frac{j2\pi nl}{N}} e^{-\theta_{l,0}} \tag{8}$$

where $D(l)$ is the clipping distortion and N is the total number of the subcarriers

$$\begin{aligned} D(l) &= \sum_{n=0x(n)<0}^{N-1} x(n)\, e^{-\frac{j2\pi nl}{N}} e^{-\theta_{l,0}} \\ &= \sum_{n=0x(n)<0}^{N/2-1} x(n)\, e^{-\frac{j2\pi nl}{N}} e^{-j\theta_{l,0}} + \sum_{n=N/2x(n)<0}^{N-1} x(n)\, e^{-\frac{j2\pi nl}{N}} e^{-j\theta_{l,0}} \end{aligned} \tag{9}$$

First, by using the odd ACO-OFDM property $x(n + \frac{N}{2}) = x(\frac{N}{2} - n)$ and changing the variables. It can be shown that

$$D(l) = \sum_{n=0x(n)<0}^{N/2-1} x(n)\, e^{-\frac{j2\pi nl}{N}} e^{-j\theta_{l,0}e^{-j\pi l}} + \sum_{l=N/2x(n)<0}^{N-1} x(n)\, e^{-\frac{j2\pi nl}{N}} e^{-j\theta_{l,0}} e^{j\pi l} \tag{10}$$

where

$$\theta_{l,0} = \frac{\pi}{2} * l$$

Table 1 Even and Odd subcarriers

	Even subcarriers	Odd subcarriers
$\cos(\frac{3\pi l}{2})$	$(-1)^{\frac{l}{2}}$	0
$\cos(\frac{\pi l}{2})$	$(-1)^{\frac{l}{2}}$	0
$\sin(\frac{3\pi l}{2})$	0	$-(-1)^{\frac{l-1}{2}}$
$\sin(\frac{\pi l}{2})$	0	$(-1)^{\frac{l-1}{2}}$

$$\begin{aligned} D(l) = &\sum_{n=0(x(n)>0}^{N/2-1} x(n)\bigg(\cos(\frac{2\pi nl}{N}) - j*\sin(\frac{2\pi nl}{N})\bigg)\times\bigg(\cos(\frac{3\pi l}{2}) - j*\sin(\frac{3\pi l}{2})\bigg) \\ &+ \sum_{l=N/2x(n)>0}^{N-1} x(n)\ \bigg(\cos(\frac{2\pi nl}{N}) - j*\sin(\frac{2\pi nl}{N})\bigg)\times\bigg(\cos(\frac{\pi l}{2}) + j*\sin(\frac{\pi l}{2})\bigg) \end{aligned} \tag{11}$$

So real part of the distortion equals

$$\begin{aligned} Re(D(l)) = &\sum_{n=0(x(n)>0}^{N/2-1} x(n)\bigg(\cos(\frac{3\pi l}{2})\times\cos(\frac{2\pi nl}{N}) - \sin(\frac{2\pi nl}{N})\times\sin(\frac{3\pi l}{2})\bigg) \\ &+ \sum_{l=N/2x(n)>0}^{N-1} x(n)\ \bigg(\cos(\frac{\pi l}{2}\times\cos(\frac{2\pi nl}{N}) + \sin(\frac{2\pi nl}{N}))\times\sin(\frac{\pi l}{2})\bigg) \end{aligned} \tag{12}$$

Substituting using values in table 1 for even subcarriers l

$$Re(D(l)) = \bigg(\sum_{n=0(x(n)>0}^{N/2-1} x(n)\cos(\frac{2\pi nl}{N}) + \sum_{l=N/2x(n)>0}^{N-1} x(n)\ \cos(\frac{2\pi nl}{N}))\bigg)\times(-1)^{\frac{l}{2}} \tag{13}$$

similarly for odd subcarriers l

$$Re(D(l)) = \bigg(\sum_{n=0(x(n)>0}^{N/2-1} x(n)\sin(\frac{2\pi nl}{N}) + \sum_{l=N/2x(n)>0}^{N-1} x(n)\ \sin(\frac{2\pi nl}{N}))\bigg)\times(-1)^{\frac{l-1}{2}} \tag{14}$$

and imaginary part of the distortion equals

$$\begin{aligned} Im(D(l)) = &\sum_{n=0(x(n)>0)}^{N/2-1} x(n)\bigg(-\sin(\frac{3\pi l}{2})*\cos(\frac{2\pi nl}{N}) - \cos(\frac{3\pi l}{2})*\sin(\frac{2\pi nl}{N})\bigg) \\ &+ \sum_{l=N/2(x(n)>0)}^{N-1} x(n)\bigg(\sin(\frac{\pi l}{2})*\cos(\frac{2\pi nl}{N}) - \cos(\frac{\pi l}{2})*\sin(\frac{2\pi nl}{N})\bigg) \end{aligned} \tag{15}$$

Substituting using values in table 1 for even subcarriers l

$$Im(D(l)) = \bigg(-\sum_{n=0(x(n)>0}^{N/2-1} x(n)\sin(\frac{2\pi nl}{N}) - \sum_{l=N/2x(n)>0}^{N-1} x(n)\ \sin(\frac{2\pi nl}{N}))\bigg)\times(-1)^{\frac{l}{2}} \tag{16}$$

similarly for odd subcarriers l

$$Im(D(l)) = \bigg(\sum_{n=0(x(n)>0}^{N/2-1} x(n)\cos(\frac{2\pi nl}{N}) + \sum_{l=N/2x(n)>0}^{N-1} x(n)\ \cos(\frac{2\pi nl}{N}))\bigg)\times(-1)^{\frac{l-1}{2}} \tag{17}$$

where

$$X(l) = -D(l) + X_{clipped}(l) \tag{18}$$

for even subcarriers X(l)=0

$$X_{clipped}(l) = -D(l) \tag{19}$$

for odd subcarriers Re(X(l))=0

$$Re(X_{clipped}(l)) = -Re(D(l)) \tag{20}$$

and

$$Im(X(l)) = Im(X_{clipped}(l)) + Im(D(l)) \tag{21}$$

substituting in equ.10

$$Im(X_{clipped}) = \sum_{n=0(x(n)>0}^{N-1} x(n)\cos(\frac{2\pi nl}{N}) \tag{22}$$

From equ. 19 and equ.24

$$Im(D(l)) = (-1)^{\frac{l-1}{2}} * Im(X_{clipped}) \tag{23}$$

$$= Im(X_{clipped}) \tag{24}$$

as $(-1)^{\frac{l-1}{2}} = -1$ for odd l

$$Im(X(l)) = \frac{Im(X_{clipped}(l))}{2} \tag{25}$$

As proved odd ACO-FBMC frames have distortion at the even subcarriers components and the real part of the odd subcarriers, Whereas the imaginary part of the odd subcarriers (loaded by the data) are not affected by the clipping distortion. So the clipping distortion causes only inter-frame interference as it has distortion on the imaginary component of the even subcarriers of the even adjacent ACO-FBMC. Similarly, it can be proved that for even ACO-FBMC frames, the clipping causes inter-frame interference on the imaginary component of the odd subcarriers of the odd adjacent ACO-FBMC.

4 SIMULATION AND RESULTS

This section shows the simulation results of the ACO-FBMC signal transmission. The total number of subcarriers is set at $L = 32$. All simulations were performed on Matlab based on Monte Carlo simulations with $10,000$ in iterations. In each iteration, the system transmits 8 frames, each separated by $\frac{T}{2}$, where T is the duration of the frame. In the first place, the clipping distorted by the receiver is measured by transmitting and detecting signals over the flat channel. As shown in Fig. 9, the signal received after the second iteration of the distortion cancelation has better performance than the signal obtained after the first iteration.

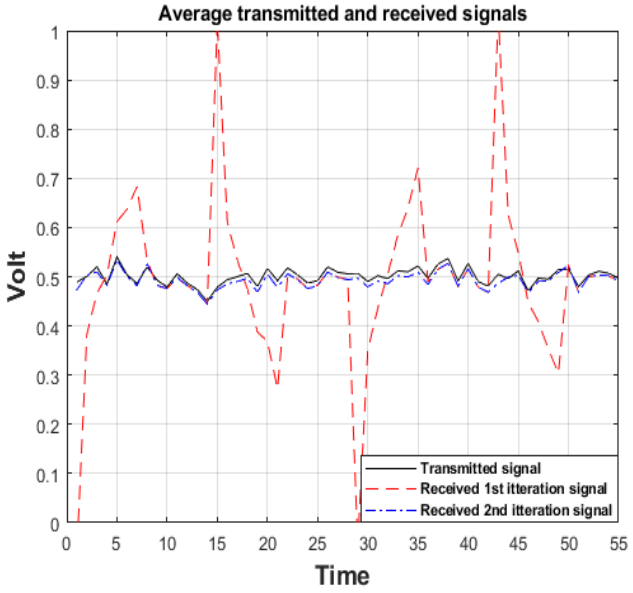

Fig. 9 Average transmitted and received signals

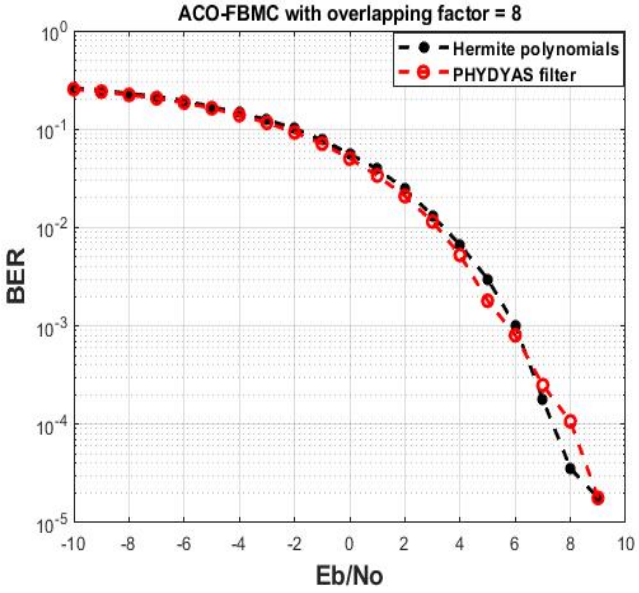

Fig. 10 BER of ACO-FBMC Hermit and PHYDYAS filter

Secondly, the BER performance of the ACO-FBMC scheme over additive white Gaussian noise (AWGN) is studied using Hermit [12] and PHYDYAS [13] filter, as shown in Fig. 10. The hermit filter shows better BER performance by only 0.5 dB. Fig. 11 shows the bit error rate (BER) of ACO-FBMC frames with an overlapping factor of 8 and the ACO-OFDM. As shown, the FBMC enhances the BER performance by 4 dB over the ACO-OFDM scheme as the filter bank shapes the transmitted signal as perfectly rectangular and eliminates the out of band emission. Furthermore, it enhances spectral efficiency due to CP cancellation. Fig. 12 shows the overlapping factor on the BER performance as the overlapping factor of 8 presents the BER performance, as the overlapping factor O characterizes the filter bank and gives different filter windows [14]. Increasing the overlapping factor narrows the filter window and increases the robustness to the inter-frame interference, enhancing the BER performance. On the other hand, it increases system complexity.

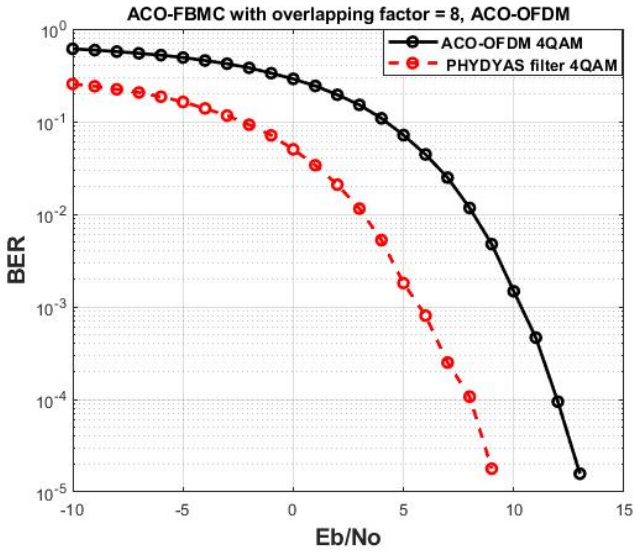

Fig. 11 BER of ACO-FBMC with 8 overlapping factor and ACO-OFDM

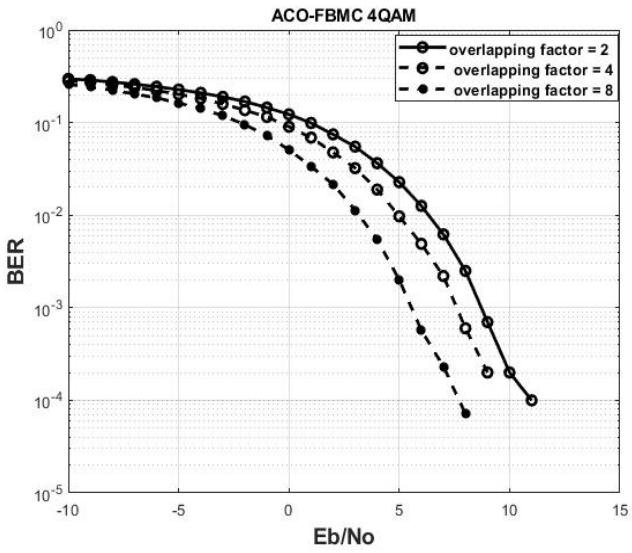

Fig. 12 BER of ACO-FBMC with 2,4,8 overlapping factor

5 CONCLUSION

The optical ACO-FBMC scheme for direct detection modulation was presented. We have shown that the proposed scheme eliminates self-frame interference and suffers from inter-frame interference. Interframe interference is eliminated using the proposed iterative receiver. Our transceiver model is based on an FFT operation and an iterative receptive method to reduce the clipping distortion. The proposed ACO-OFDM removed the guard interval, which increased spectral efficiency. Also, the ACO-FBMC enhances the BER performance of the ACO-OFDM with the perfect rectangular pulse shaping and eliminating the emission of the filter bank out of the band. Our system model has higher spectral efficiency than the classic ACO-OFDM, as FBMC shows better spectral efficiency by removing the guard interval. Moreover, it has been shown that the ACO-FBMC with 8 overlapping factors improves the BER performance of the ACO-OFDM by 4 dB due to the perfect rectangular pulse shaping and the elimination of the out-band emission of the filter bank.

Declaration

We are enclosing herewith a manuscript entitled “Asymmetrical Clipping Optical Filter Bank Multi-carrier Modulation Scheme” for publication in Optical and Quantum Electronics Journal.

With the submission of this manuscript I would like to undertake that: - All authors of this research paper have directly participated in the planning, execution, or analysis of this study; - All authors of this paper have read and approved the final version submitted; - The contents of this manuscript have not been copyrighted or published previously; - The contents of this manuscript are not now under consideration for publication elsewhere; - The contents of this manuscript will not be copyrighted, submitted, or published elsewhere, while acceptance by the Journal is under consideration; - There are no directly related manuscripts or abstracts, published or unpublished, by any authors of this paper.

Conflict of interest

Manuscript title:

Asymmetrical Clipping Optical Filter Bank Multi-carrier Modulation Scheme.

The authors whose names are listed immediately below certify that they have NO affiliations with or involvement in any organization or entity with any financial interest (such as honor-aria; educational grants; participation in speakers’ bureaus; membership, employment, consultancies, stock ownership, or other equity interest; and expert testimony or patent-licensing arrangements), or non-financial interest (such as personal or professional relationships, affiliations, knowledge or beliefs) in the subject matter or materials discussed in this manuscript.

Author names:

Asmaa Ibrahim, Josep Prat and Tawfik Ismail

References

1. C. Ranaweera, E. Wong, A. Nirmalathas, C. Jayasundara and C. Lim, "5G C-RAN With Optical Fronthaul: An Analysis From a Deployment Perspective," in Journal of Lightwave Technology, vol. 36, no. 11, pp. 2059-2068, 1 June, 2018.
2. P. Iovanna, F. Cavaliere, F. Testa et al., "Future proof optical network infrastructure for 5G transport," Journal of Optical Communications and Networking, vol. 8, no. 12, p. B80, 2016.
3. A. Sahin, I. Güvenç, and H. Arslan, "A survey on multicarrier communications: Prototype filters, lattice structures, and implementation aspects," IEEE Communication Surveys and Tutorials, Dec. 2013.
4. P. Siohan, C. Sicletand, and N. Lacaille, "Analysis and design of OFDM/OQAM systems based on filter bank theory," IEEE Transaction of Signal Processing, vol. 50, pp. 1170-1183, May 2002.
5. R. Chen, K.-H. Park, C. Shen, T. K. Ng, B. S. Ooi, and M.-S. Alouini, "Visible light communication using DC-biased optical filter bank multicarrier modulation," in Proc. Global LIFI Congress (GLC), Paris, France, Feb. 2018.
6. R. Nissel, S. Schwarz, and M. Rupp, "Filter bank multicarrier modulation schemes for future mobile communications," IEEE J. Sel. Areas Commun., vol. 35, no. 8, pp. 1768–1782, Aug. 2017.
7. H. Lin and P. Siohan, "OFDM/OQAM with hermitian symmetry: Design and performance for baseband communication," in IEEE International Conference on Communications, (ICC '08), pp. 652–656, Beijing 2008.
8. A. Ibrahim, T. Ismail, K. Elsayed and M. Saeed, "Odd Clipping Optical Orthogonal Frequency Division Multiplexing for VLC System," International Journal of Communication Systems, Wiley, e3942, vol. 32, no. 16, Sep. 2019.
9. H. Elgala, R. Mesleh, and H. Haas, "Indoor broadcasting via white LEDs and OFDM," in IEEE Transaction Consumer Electronics, vol. 55, no. 3, pp. 1127-1134, 2009.
10. S. Dissanayake and J. Armstrong, "Comparison of ACO-OFDM, DCOOFDM and ADO-OFDM in IM/DD systems," in Journal of Light Wave Technology, vol. 31, no. 7, pp. 1063-1072, 2013.
11. S. Sarmiento, J. A. Altabas, S. Spadaro, and J. A. Lazaro, "From 4.2Gbps Asymmetrical Clipping (ACO)-OFDM to 8.7Gbps Layered-ACO-FBMC with Intensity-Modulation Direct-Detection for PONs," in 2019 Conference on Lasers and Electro-Optics Europe and European Quantum Electronics Conference, OSA Technical Digest (Optical Society of America, 2019).
12. R. Haas and J.-C. Belfiore, "A time-frequency well-localized pulse for multiple carrier transmission," Wireless Personal Communications, vol. 5, no. 1, pp. 1–18, 1997.
13. M. Bellanger, D. Le Ruyet, D. Roviras, M. Terre, J. Nossek, L. Baltar, Q. Bai, D. Waldhauser, M. Renfors, T. Ihalainen et al., "FBMC physical layer: a primer," PHYDYAS, January, 2010.
14. H.A. Ali, R.M. Zaki, M.M. Tantawy, "Overlapping factor effect on the prototype filter response proposed for FBMC trans multiplexer system," ICENCO 2018 - 14th International Computer Engineering Conference, 2019.